34th Annual International Conference of the IEEE EMBS
San Diego, California USA, 28 August - 1 September, 2012

A coding scheme for optoelectronic/optogenetic retinal prosthesis

Patrick Degenaar, Walid Al Atabany

***Abstract*—The field of retinal prosthesis has been steadily developing over the last two decades. Despite the many obstacles, clinical trials for electronic approaches are in progress and already demonstrating some success. Optogenetic/optoelectronic retinal prosthesis may prove to have even greater capabilities. Although resolutions are now moving beyond recognition of simple shapes, it will nevertheless be poor compared to normal vision. If we define the aim to be to return mobility and natural scene recognition to the patient, it is important to maximize the useful visual information we attempt to transfer. In this work we highlight a method to simplify the scene, perform spatial image compression and a pulse coding scheme on the optoelectronic stimulator to conserve energy consumption.**

***Index Terms*— retinal prosthesis, optogenetics, visual prosthesis, scene enhancement, augmented vision, optoelectronics, channelrhodopsin**

I. Introduction

The sense of vision is incredibly important to human beings. Much of our daily existence from internet browsing to navigation presupposes our ability to see. Its loss can therefore be devastating. Surgical approaches have been developed for optical conditions such as cataracts, and drugs are becoming increasingly available for conditions such as wet Age-related Macular Degeneration. However, genetic disorders of the retina are much more difficult to treat. In Retinitis Pigmentosa (RP), defective rod photoreceptors cause nightblindness and tunnel vision. As the disease progresses, cone photoreceptors become inactivated and eventually destroyed. The circuitry of the retina is however largely intact [1].

Despite the successes of cochlear implants, the retina has proved to be very challenging to neuroprostheticists. Progress therefore has been slow [2, 3]. However with the advent of optogenetics in 2003, a new form of optogenetic/optoelectronic prosthesis has been conceptualized by this team [4] and others. Fundamentally, this new approach photosensitizes other cells in the retina with a light sensitive ion channel. This has been shown in retinal ganglion cells [5], bipolar cells [6]. It also turns out that even after the onset of full blindness, many of the photoreceptor cells in the central macula, though dysfunctional, remain alive. It is thus possible to re-sensitize these with photosensitive ion pumps [7]. The main caveat to this approach is the requirement for ultra bright light sources – typically emitting at 10^6 cd/m^2. To this end we have been developing high brightness microLED array technology [8] which can provide high brightness stimulus at high pulse frequencies.

The key advantage to optogenetic approaches relate to not requiring implantation of electrodes, which degrade, and the inherently higher resolution and contrast achievable. In particular it is possible to genetically target neural pathways. [6], and even re-photosensitize the cone cells. The key engineering caveat is that a very high intensity of light – typically 1mW/mm^2 is required to stimulate the target cells. Realistically, perhaps not all of the re-sensitized cells may be functional, and those that are exist only in the fovea. As such the returned vision may look like that given in Figure 1 below.

Given the intensity requirements and the non-perfect returned vision, we need to create a scheme which maximizes the useful transfer of information while minimizing energy consumption. Previously, we have shown that effective contrast enhancement algorithms such as cartoonization and TRON can improve visual recognition in low-vision patients with retinal degenerative disorders [9]. For those with tunnel vision, we have also demonstrated a non-linearly shrinking approach [10] to spatially compress the non important features of the visual scene, increasing the effective field of view.

Figure 1 optogenetic vision. (left) original scene (right) simulated optogenetic vision. Not all cone cells will have returned function so there will be a scatter. Also, as only the foveal cones will remain, there will be a tunnel vision.

In this paper we combine cartoonization to improve effective contrast, with our spatial scene compression algorithm and a power management method to limit the power consumed by the micro-LED arrays[11].

II. Processing Algorithms

The visual processing is divided into three main parts described in the flow chart in Figure 2:

1. Scene simplification: to reduce the non-important features and increase effective contrast.

2. Spatial scene compression: To shrink the scene while maintaining the important components to fit more information into the visual tunnel.

3. MicroLED pulse coding: To ensure smoothing of the

power consumption and limit the total power consumed.

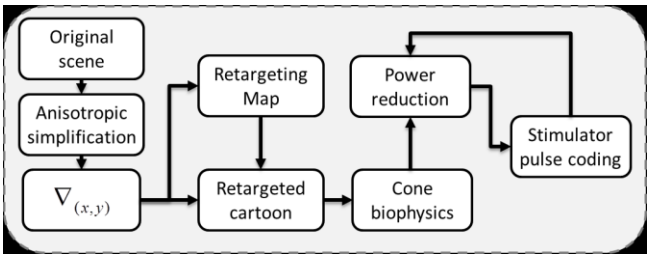

Figure 2 System flowchart. It shows the main stages of the approach for stimulating re-sensitized Cone target. The retargeted simplified cartoon scene will be transmitted to a module encoding for the cone biophysics and the microLED encoding.

A. Spatial contrast enhancement

The purpose here is to suppress non important high frequency noise and textures. We use an anisotropic diffusion filter to eliminate noise and low importance textures, while avoiding smoothing across object boundaries [12]. The discrete equation of this filter is:

$$I^{n+1} = I^n + \Delta t \sum \begin{bmatrix} \nabla(C \cdot \nabla I_H) & \nabla(C \cdot \nabla I_V) \\ \nabla(C \cdot \nabla I_{D1}) & \nabla(C \cdot \nabla I_{D2}) \end{bmatrix} \quad (1)$$

Where ∇ is the gradient operator and C is the diffusion coefficient or the diffusivity of the equation. n denotes the iteration number, Δt is the time step (it controls the accuracy and the speed of the smoothing) and ∇I_H, ∇I_V, ∇I_{D1} and ∇I_{D2} represent the horizontal (H), vertical (V), and two diagonal (D) gradients of the image. We achieve this with Sobel operators. The diffusion coefficient C is calculated from the following equation.

$$C = \frac{1}{1 + \sqrt{\nabla I_H^2 + \nabla I_V^2 + \nabla I_{D1}^2 + \nabla I_{D2}^2}} \quad (2)$$

To increase the visual distinctiveness of high contrast regions in the scene, we overlay a negative spatial derivative over simplified scene which gives a notable edge enhancement giving the image a cartoon like effect.

B. Spatial scene compression

Simple bilinear resizing of the visual scene would make key features seem further away [13]. This makes the object identification process more difficult at lower spatial resolution. We therefore need to non-linearly retarget the scene into a smaller size, thus expanding the effective field of vision. To do that we have developed a non-linear scene retargeting technique, which generates an importance matrix W_{ST} this involves how much each pixel in the input scene should be nonlinearly shrunk (comprised). It is a combination of two measures: a local saliency gradient map, and a temporal motion map. The later is derived from a temporal derivative of the visual scene:

$$W_{ST} = \nabla(x,y,t) + \frac{1}{2n}\sum_{n=1}^{N}\frac{1}{n}(\nabla(x,y,t) - \nabla(x,y,t-n) \quad (3)$$

We use n=1 to minimize processing requirement. To give higher importance values for the foreground objects over the saliency and background objects, we modify the importance matrix by giving background areas very low importance weights. The modification process starts by looking for seams with lowest cumulative energy values [10, 14]. A seam is defined to be a connecting path of pixels (one in each row, in case of vertical compression) with minimum energy values. By knowing the locations of lowest energy pixels, we rescale all the pixels of the importance matrix along the path of all the seams to very low importance values.

The importance matrix ranks the components of the scene. The shrinkability matrix defines the relative extent to which pixels in the source image should be shrunk to retarget the image by K columns. The shrinking value of each pixel $S(j)$ for row or column shrinkage is given by:

$$S(j) = \frac{1}{W(j) * \sum_{j=1}^{M} 1/W(j)} \quad (4)$$

(The summation of $S(j)$ over j columns equals K. The adaptation of the importance matrix and the shrinkage map processes are fully discussed in our previous paper [10].

C. Cone biophysics and pulse coding.

Cone cells are analog signal integrators which determine signal intensity and module glutamate release accordingly. From the literature [7], we determine the cone cell response to light to be as follows:

$$R = \frac{\phi}{50}^{0.4} \quad (5)$$

Where R is the cell response and ϕ is the light intensity. As such we rescale our image to take this into account and reset to a given dynamic range. As the light is pulse width modulated, the dynamic range is a given frame time divided by the minimum pulse time. Generally in virtual reality we need frames time less than 20ms (i.e.> 50Hz) to prevent motion sickness. We can also presently address our LED array within 1ms but hope to scale that to 100µs in the near future. We have therefore used a dynamic range of 200.

The photon dynamic range of the cells is 10^{15}-10^{17} Photons/cm^2 [7]. This equates to a requirement of 3x10^{-5}-10^{-3}W/mm^2. Typically, our LEDs are 1% efficient, and we assume the same for the optics. We therefore require an energy consumption of 0.3-30W/mm2 from our emission system. Each pixel is 100µm^2 and will therefore consume between 3-300 µW. We have therefore introduced a recursive algorithm to prevent the energy consumption becoming too high.

Once we have determined our dynamic range, we convert to a pulse width modulation scheme and distribute the 100µs pulses evenly through 20ms time space. As there is a range of different brightness, there will then be a reduced probability of all LEDs being turned on at once. A check is put in place whereby should the predicted output go beyond

the power threshold, the dynamic range is reduced accordingly.

D. Implementation

The prototyping platform has been implemented on a desktop computer; with a 2.8 GHz Intel Core Quad processor, 8 Gb Memory, and a GTX285 graphics card. The program was written in Matlab with an Accerlereyes GPU plug-in and connected via USB to our microLED array. An image of our set up can be seen in Figure 3 below.

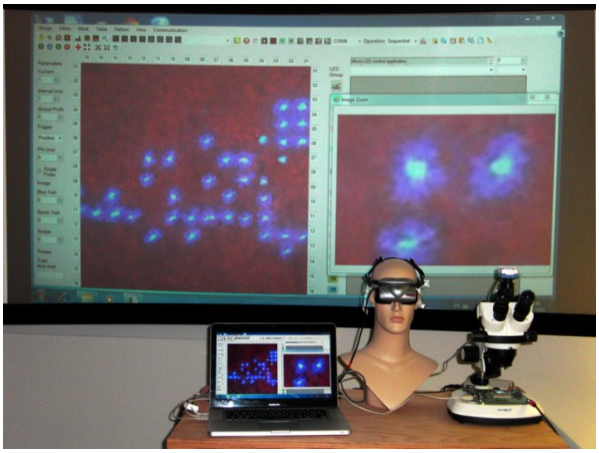

Figure 3 Snapshot from the experiment. A snapshot for the whole system describing the main components, Left, a computer system performing the processing, centre a virtual reality helmet camera on a dummy, right the microLEDs analyzed under a microscope.

III. Results and Discussion

To demonstrate the effect of scene simplification, we performed the cartoonization step on a low contrast scene. The results are shown in Figure 4, and the cartoonized versions clearly show improvement in our model of returned vision.

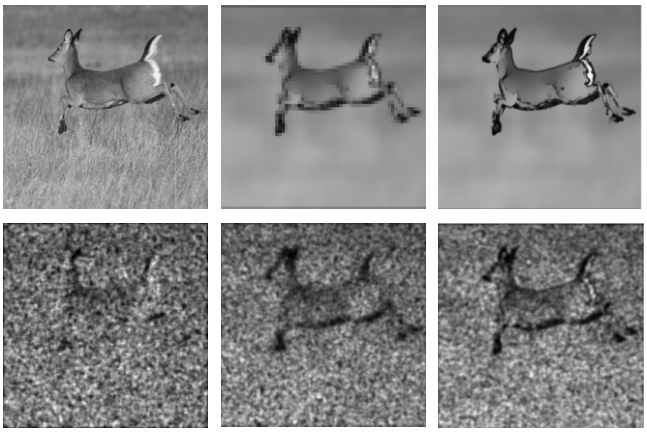

Figure 4 The effect of scene simplification Top row from left to right: a 256x256 image of a low contrast scene, 64x64 cartoonized version, and a 256x256 cartoonized version. The bottom row shows our estimation of how it would be perceived assuming 30% of the resensitized cone cells are functional.

Figure 5, shows a snapshot from video file for subjects moving in playground field with dimension of 400×400. The images have been left in edge form for ease of dimension comparison. The scene is retargeted using three methods; our seam-assisted-shrinkability (SAS) retargeting approach (first row of Figure 5 (B)), bilinear resizing (second row) and cropping (last row).

The SAS method cannot know future scenes, so it exhibits an increasing wobble or video jitter with higher spatial compressions. Subjectively we find a 25-40% compression gives the most effective result [10]. We therefore show comparative compressed images of 256×256 pixels for each of the cases, which are then interpolated to 64×64 and 16×16 pixels. Image cropping (tunnel vision) loses peripheral information, and resizing makes objects seem further away. The SAS algorithm compresses the less useful information keeping the main features at the same size.

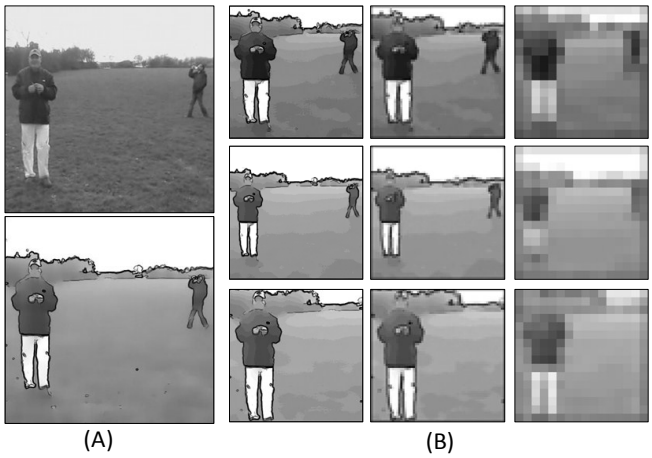

Figure 5 The effect of different retargetting techniques (A) The image before and after cartoonization (bottom). (B) First, Second and third rows in show the retargetd image to 256×256, 64×64 and 16×16 (from left to right) when using our retargeting, simple bilinear resizing and croping methods, respectively.

Our LED stimulator is pulse modulated. For intensity modulation of the re-sensitized cone cells, we simply vary the pulse within the cells integral period (~20ms).

At present the pulse width is determined by the brightness/efficiency of the micro-LED stimulator and the efficiency of the channelrhodopsin. Already a CatCh[15] form of channelrhodopsin shows significantly improved light requirement and we expect further improvements in the coming years. Similarly, we expect to improve the external quantum efficiency of the microLED stimulator. In practice, this will reduce the required stimulation pulse width. Reducing the width of the stimulating pulse increases the number of the allowed stimulating spikes. This in turn enhances the visual perceived scene for larger image sizes (e.g. 256×256)

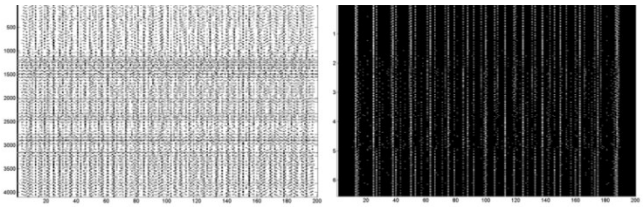

Figure 6 Pulse distribution from the microLEDs using PWM intensity control. Left the light pulse distribution from a 64x64 array. Right, the pulse distribution from a 256x256 array.

Our results showed the importance of scene simplification and retargeting approaches before transferal to the patient. We conclude that subjectively, a 25-40% spatial compression of the image from the original size can give acceptable results [10].

Although we believe the µLED array will be the dominant power consumer, it will be important to minimize processing energy requirement. Although we have implemented on a PC, our algorithms are scalable to mobile processing devices. The estimated power consumption of the final system will be limited to around 1W. A typical mobile phone battery is capable of ~5 Whrs. Thus, perhaps 4 such batteries would power the required processing over the course of a day. Although it is interesting to note, as we develop every larger µLED arrays, there may be a tradeoff between image dynamic range and resolution in order not to overload the circuitry. But again, as the efficiency of both the microLED illuminator and the channelrhodopsin biophysics improves, the power requirement will be decreased.

IV. Conclusion

We have shown in this paper the scene pre-processing steps needed to be used in an in-vivo system to stimulate arrays of genetically re-sensitized cone cells using light. The aim of this pre-processing is to enhance and maximize the visual information included in the scene before spike coding and sending it to the retina. We demonstrated how the scene simplification and our non-linearly retargeting technique kept the relevant information of the scene when it is downscaled to small scales. We also showed that we can modify the pulse width modulation scheme to smooth the current usage and trade-off between power consumption and dynamic range.

References

[1] J. L. Stone*, et al.*, "Morphometric Analysis of Macular Photoreceptors and Ganglion-Cells in Retinas with Retinitis-Pigmentosa," *Archives of Ophthalmology,* vol. 110, pp. 1634-1639, Nov 1992.

[2] M. S. Humayun*, et al.*, "Preliminary 6 Month Results from the Argus (TM) II Epiretinal Prosthesis Feasibility Study," *Embc: 2009 Annual International Conference of the Ieee Engineering in Medicine and Biology Society, Vols 1-20,* pp. 4566-4568, 2009.

[3] E. Zrenner*, et al.*, "Subretinal electronic chips allow blind patients to read letters and combine them to words," *Proceedings of the Royal Society B-Biological Sciences,* vol. 278, pp. 1489-1497, May 22 2011.

[4] P. Degenaar*, et al.*, "Optobionic vision--a new genetically enhanced light on retinal prosthesis," *Journal of Neural Engineering,* vol. 6, p. 035007, Jun 2009.

[5] A. D. Bi*, et al.*, "Ectopic expression of a microbial-type rhodopsin restores visual responses in mice with photoreceptor degeneration," *Neuron,* vol. 50, pp. 23-33, Apr 6 2006.

[6] P. S. Lagali*, et al.*, "Light-activated channels targeted to ON bipolar cells restore visual function in retinal degeneration," *Nature Neuroscience,* vol. 11, pp. 667-675, Jun 2008.

[7] V. Busskamp*, et al.*, "Genetic Reactivation of Cone Photoreceptors Restores Visual Responses in Retinitis Pigmentosa," *Science,* vol. 329, pp. 413-417, Jul 23 2010.

[8] B. McGovern*, et al.*, "A New Individually Addressable Micro-LED Array for Photogenetic Neural Stimulation," *Ieee Transactions on Biomedical Circuits and Systems,* vol. 4, pp. 469-476, Dec 2010.

[9] W. Al-Atabany*, et al.*, "Designing and testing scene enhancement algorithms for patients with retina degenerative disorders," *BioMedical Engineering OnLine,* vol. 9, p. 27, 2010.

[10] W. Al-Atabany*, et al.*, "Improved content aware scene retargeting for retinitis pigmentosa patients," *BioMedical Engineering OnLine,* vol. 9, p. 52, 2010.

[11] W. Al-Atabany*, et al.*, "A processing platform for optoelectronic/optogenetic retinal prosthesis," *IEEE Trans Biomed Eng,* Nov 24 2011.

[12] P. Perona and J. Malik, "Scale-Space and Edge-Detection Using Anisotropic Diffusion," *Ieee Transactions on Pattern Analysis and Machine Intelligence,* vol. 12, pp. 629-639, Jul 1990.

[13] N.Sharmili*, et al.*, "Image Compression and Resizing for Retinal Implant in Bionic Eye," *International Journal of Computer Science & Engineering Survey (IJCSES),* vol. 2, pp. 30-37, 2011.

[14] A. Shai and S. Ariel, "Seam carving for content-aware image resizing," *ACM Trans. Graph.,* vol. 26, p. 10, 2007.

[15] E. Bamberg*, et al.*, "Ultra light-sensitive and fast neuronal activation with the Ca(2+)-permeable channelrhodopsin CatCh," *Nature Neuroscience,* vol. 14, pp. 513-U152, Apr 2011.

We would like to thank the European FP7 program for funding the OptoNeuro (249867) research program. Dr. Walid Al Atabany would also like to thank the Egyptian government for research funding during his recently completed PhD program.

Patrick Degenaar is with the School of Electrical and Electronic Engineering, and the Institute of Neuroscience, both at the University of Newcastle, Newcastle upon Tyne, NE1 7RU, UK (e-mail: patrick.degenaar@newcastle.ac.uk).

Walid Al Atabany is with the School of Electrical and Electronic Engineering, and the University of Newcastle, UK, and Department of Biomedical Engineering, Helwan University, Egypt